

1 Article

2 Case study: Spiking neural network hardware 3 system for structural health monitoring

4 Lili Pang ^{1,*}, Junxiu Liu ^{2,*}, Jim Harkin ², George Martin ², Malachy McElholm ², Aqib Javed ², and
5 Liam McDaid ²

6 ¹ Industrial Center/School of Innovation and Entrepreneurship, Nanjing Institute of Technology, Nanjing
7 211167, China; panglili@njit.edu.cn

8 ² School of Computing, Engineering and Intelligent Systems, Ulster University, UK; {j.liu1, jg.harkin,
9 gs.martin, m.mcelholm, javed-a, lj.mcdaid}@ulster.ac.uk

10 * Correspondence: panglili@njit.edu.cn (LP), j.liu1@ulster.ac.uk (JL)

11 Received: date; Accepted: date; Published: date

12 **Abstract:** This case study provides feasibility analysis of adapting Spiking Neural Networks (SNN)
13 based Structural Health Monitoring (SHM) system to explore low-cost solution for inspection of
14 structural health of damaged buildings which survived after natural disaster i.e., earthquakes or
15 similar activities. Various techniques are used to detect the structural health status of a building for
16 performance benchmarking, including different feature extraction methods and classification
17 techniques (e.g. SNN, K-means and artificial neural network etc.). The SNN is utilized to process
18 the sensory data generated from full-scale seven-story reinforced concrete building to verify the
19 classification performances. Results show that the proposed SNN hardware has high classification
20 accuracy, reliability, longevity, and low hardware area overhead.

21 **Keywords:** Structural Health Monitoring; Damage State Classification; Spiking Neural Networks;
22 Feature Extraction; Artificial Neural Networks

23

24 1. Introduction

25 Earthquake is an oscillatory movement caused by abrupt release of strain energy stored in in the
26 rocks within the crust of earth surface. Natural disasters are always vulnerable which leads to
27 extreme damages in nearby population in terms of fatality, communication and infrastructure loss.
28 Flood, earthquake, cyclones etc. are among most common occurring natural disasters across world.
29 The impact of these disasters differs in geological and geographic location of an area. These disasters
30 come with no advance warning but an effective, well prepared and maintained infrastructure will
31 decrease potential impact of future disasters. The structural health of buildings and other
32 infrastructures suffers degradation due to environmental catastrophes caused by ageing, hazards and
33 natural disasters [1]. In any area, public infrastructures like school, hospital, fire station,
34 administrative buildings, bridges, treatment plants are more prone to be highly affected by these
35 disasters. Therefore, regular structural health monitoring is required to ensure health and endurance
36 from these mega structures. In an event of disaster, it is particularly important i). to detect and
37 quantify the severity of damage caused by environmental disasters at an early stage, ii). to assess the
38 current structural health and reliability of buildings to ensure its safe use, and iii) to estimate
39 repairing cost for damage to minimize economic losses [2]. Traditional monitoring methods rely on

40 an inspection and assessment of the buildings and requires experienced inspectors. Many structures
41 are not convenient for on-site monitoring due to the terrain obstacles i.e., lack of access to such
42 buildings and which sometimes makes it too late due to the retrospective nature of inspections [3].
43 An automated process such as installation of a Structural Health Monitoring (SHM) system on
44 vulnerable structures, e.g. buildings, bridges and even special launch vehicles, to periodically detect
45 and notify structural damages [4]. An advance SHM systems should include current health profile of
46 the structure, the functions of damage detection, structural life prediction etc. [5]. The lifespan of
47 typical structure lasts for decades whereas sensory instruments and microprocessors used by SHM
48 systems comes with limited lifespan, e.g. in an ideal operating environment the three-axis
49 accelerometer of IIS3DHC from the STMicroelectronics has ten-year production life which further
50 shrinks in harsh outdoor environments. Therefore, after installation and regular use for several years
51 SHM systems may fatigue and fail. Due to technical and economic difficulties for secondary
52 deployment, the longevity and reliability of SHM systems are key challenges that must be considered.

53 Considering these issues, SHM Systems should offer three characteristics. Firstly, the system
54 should be adaptive, robust, and capable to learn quickly. Secondly, the data analysis of the SHM
55 system should be fast, efficient and accurate. Finally, the longevity and reliability of the systems
56 hardware should be enhanced as the SHM system may be deployed in harsh conditions. The SHM
57 system must has protection capabilities to resist the hazardous effect of external environment. Recent
58 research suggested that we can build human brain like fault-tolerant energy-efficient system with
59 learning capability to enhance the robustness, productivity and endurance of the electronic hardware
60 systems [6,7]. Spiking neural network (SNN) are referred as the 3rd generation of artificial neural
61 network (ANN). Contrary to conventional ANNs, SNNs are more realistic mathematical
62 representation of the human brain that mimics biological spike-based event-driven processes to
63 communicate between neurons. SNNs are computationally complex and powerful than conventional
64 ANNs [8]. On an embedded processor, this digital systems like spike-driven communication
65 capability makes SNNs i.e., astrocyte-neural network model more energy-efficient and reliable than
66 deep neural network [9]. [Therefore, this paper proposes an SHM system that based on SNN hardware
67 to address the challenges of longevity and reliability of the monitoring system. The acceleration data
68 collected from a full-scale seven-story reinforced concrete building are analyzed and severity of
69 damage in the building are subsequently classified. The proposed system can monitor and detect
70 the structure health damage levels under different environmental conditions, and provides a
71 high detection accuracy and relatively low hardware overhead for implementation.](#)

72 The following section (section 2) explores related works and briefly reviews current SHM
73 solutions and methodologies used to assess the structural health of buildings and structures. Section
74 3 defines the proposed SHM system, discusses feature analysis and classification methods for the
75 sensor data. Section 4 provides the experimental results to demonstrate the feasibility and accuracy
76 of the proposed system through actual building sensor data. Finally, section 5 concludes the paper
77 and gives the directions for future work.

78 2. Related works

79 SHM systems need to provide a framework for the damage classification using a continuous
80 record of structural health monitoring data. This classification framework requires categorization of
81 many datasets relating to different states of structural health [10]. Damage identification in SHM
82 involves four main steps: signal acquisition, signal processing, feature extraction and classification.
83 The acquired data are then analyzed by signal processing techniques to extract, identify and classify
84 key features which are used for assessing the health condition of the structure. Feature extraction and
85 classification techniques are very critical for assessment of the structural health condition in an
86 automated system. Feature extraction method focuses on extracting features which may indicate
87 damage state 'hidden' in recorded sensor data, e.g. the orthogonal decomposition method is used for
88 feature extraction and analysis [11]. Feature extraction relies on empirical data. As the structure is

89 affected by the environmental conditions, sensor data includes noises which affects damage level
90 assessment [12]. Therefore, feature extraction is a foremost and critical step for the SHM system.

91 Another challenge of SHM systems is the damage classification method. Previous research work
92 proposed various damage classification methods for different structures. Conventional classification
93 methods include clustering algorithms [13] i.e., k-means (KM) which is widely used in SHM.
94 However, KM is sensitive to the extracted data features and the initial choice of cluster centres [14]
95 that may lead to erroneous classifications [13]. ANNs has shown to be a promising technique for
96 SHM classification [9]. It includes a set of computational models inspired by the interconnected
97 neurological structure of the human brain for learning and solving problems such as pattern
98 recognitions. Taking into account the different classification rules of different structures and the use
99 of different types of sensors [15] (e.g. sensors for measuring mechanical properties [16,17] and sensors
100 for measuring environmental properties [18–20]), neural networks have the ability to extract features
101 from the data automatically [21], which can meet the requirements of applications. However, existing
102 systems are not suitable for detecting and analysing the structural characteristics in real applications
103 such as SHM, as the system cannot meet practical needs in terms of hardware cost and power
104 consumption.

105 Unlike traditional ANN, Spiking Neural Networks (SNNs) have a smaller hardware overhead
106 and are more reliable and power efficient. It has been reported that SNN hardware such as
107 neuromorphic systems consume two orders of magnitude less energy than ANNs [22]. In brain-
108 inspired intelligence research, SNNs demonstrate a low power consumption and high performance
109 for the deployment of artificial intelligence technology. In addition, if considering the glial cell such
110 as astrocyte, spiking neural astrocyte networks have shown the self-repairing capability by using a
111 novel learning rule [23]. Therefore, this work proposed an SHM solution based on SNN hardware
112 system with self-repairing capability that will improves the electronic system reliability and life-span
113 in harsh environments. To the best of the authors' knowledge, conventional ANN and Probabilistic
114 Neural Networks (PNN) are widely used for structural damage detection [24–26], but no structural
115 health monitoring application of SNN has been reported in the literature. Therefore, by combining
116 the energy-efficient SNN classification algorithm and the highly compact neural network hardware,
117 the performance and lifetime of the SHM system can be improved. Results in section 4 will
118 demonstrate the proposed work makes SHM a viable option with low energy consumption, anti-
119 noise capability, and an efficient data processing capability.

120 3. SHM system based on SNN

121 This section explores architectural components of proposed SNN based SHM system including
122 data acquisition (sensors) and decision-making mechanism (damage level classification).
123 Furthermore, benchmarks of K-means and ANN algorithms are also briefly introduced in this section.

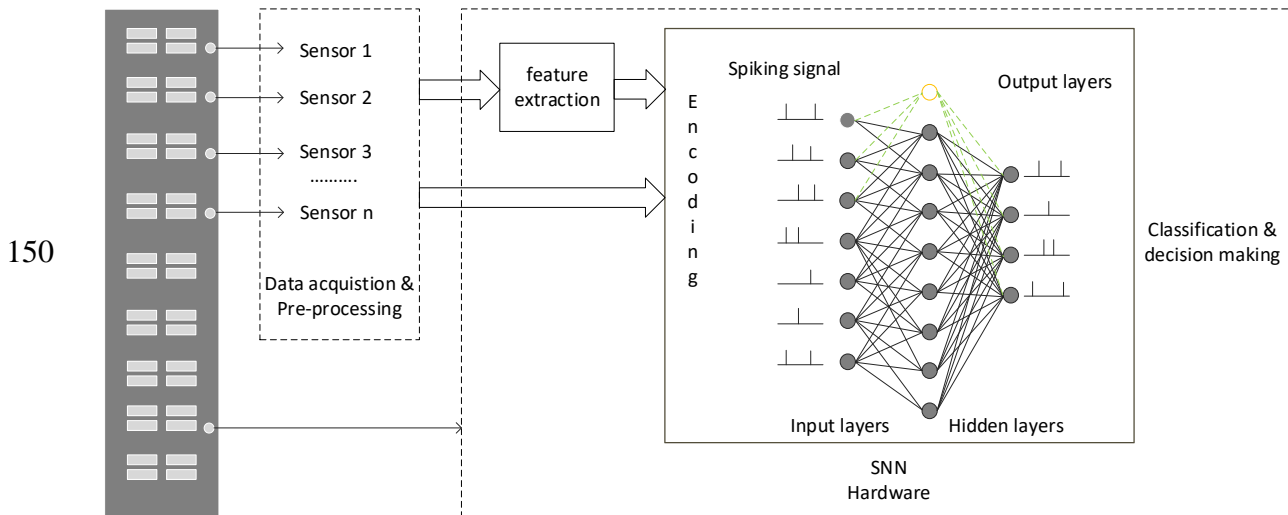
124 3.1. System architecture

125 SHM is a multi-layered hardware system that comprises up of multiple sensors for data
126 acquisition, communication and processing architecture to assess health of structural integrity. Figure
127 1 shows the structure of the proposed SHM system. System is equipped with Wired or wireless
128 sensors such as accelerometers to collect the data from under observation structure. Through the
129 analysis of the raw data, appropriate features can be selected and extracted from the time domain or
130 frequency domain. After feature extraction, the data is fed into the SNN hardware system for the
131 structure damage level assessment. The SNN encodes the pre-processed data into input spiking
132 signals. This work proposed two SNN models to explore an efficient and cost-effective solution for
133 SHM system. A fully connected SNN network based on Leaky Integrate and Fire (LIF) neurons with
134 SpikeProp as learning algorithm for feature classification. Second model is based on Neucube
135 framework [27] using the Spike Timing Dependent Plasticity (STDP) rule for the unsupervised

136 training and deSNN [28] algorithm for supervised learning. Both models can classify the level of
 137 structure damage to identify structural health status.

138 SNNs use time as an input dimension and records valuable information in a spatial domain. The
 139 information received by the spiking neuron is a pulsed time series, so the analogue sensory data
 140 needs to be encoded into spatial dimension for input to the spiking neural network. spiking neuron
 141 membrane changes upon arrival of input spike and each postsynaptic neuron fires an action potential
 142 or spike at the time when the membrane potential exceeds the firing threshold [29]. The event-driven
 143 neurons in an SNN are only active when they receive or emit spikes, which can contribute to energy
 144 efficiency over time.

145 Hardware systems that implement neuronal and synaptic computations through spike-driven
 146 communication may enable energy-efficient machine intelligence [30]. Compared with the traditional
 147 neuron model, the spiking neuron model has lower power consumption and is also suitable for
 148 parallel computing. Therefore, using a spiking neural hardware system can speed up the
 149 computation power.



151 **Figure 1.** An SNN-based SHM system

152 3.2. Feature extraction

153 Considering different sensors used in the structure, the selection of damage-sensitive features is
 154 generally based on multiple tests, so as to determine which features can indicate the health state of
 155 the structure accurately and are robust to the influence of the structural conditions and environments.
 156 These features can be extracted from the time domain (e.g. mean, variance, peak to peak amplitude,
 157 Zero crossing rate, energy, maximum amplitude, etc.), and frequency domain such as Fourier
 158 transform. Mean, variance and zero crossing rate are defined as:

$$159 \text{mean}(a) = \frac{1}{N} \sum_{i=1}^N a_i \quad (1)$$

$$160 \text{variance}(a) = \frac{1}{N} \sum_{i=1}^N (a_i - \text{mean}(a))^2 \quad (2)$$

$$161 \text{zcr}(a) = \frac{1}{N-1} \sum_{i=1}^{N-1} \Pi\{a_i a_{i-1} < 0\}, \Pi\{A\} = \begin{cases} 1 & A \text{ is true} \\ 0 & A \text{ is false} \end{cases} \quad (3)$$

159 where a is the input sensor data, N is the number of the samples. After feature extraction, supervised
 160 or unsupervised learning methods can be used for data analysis and structure health status
 161 classification.

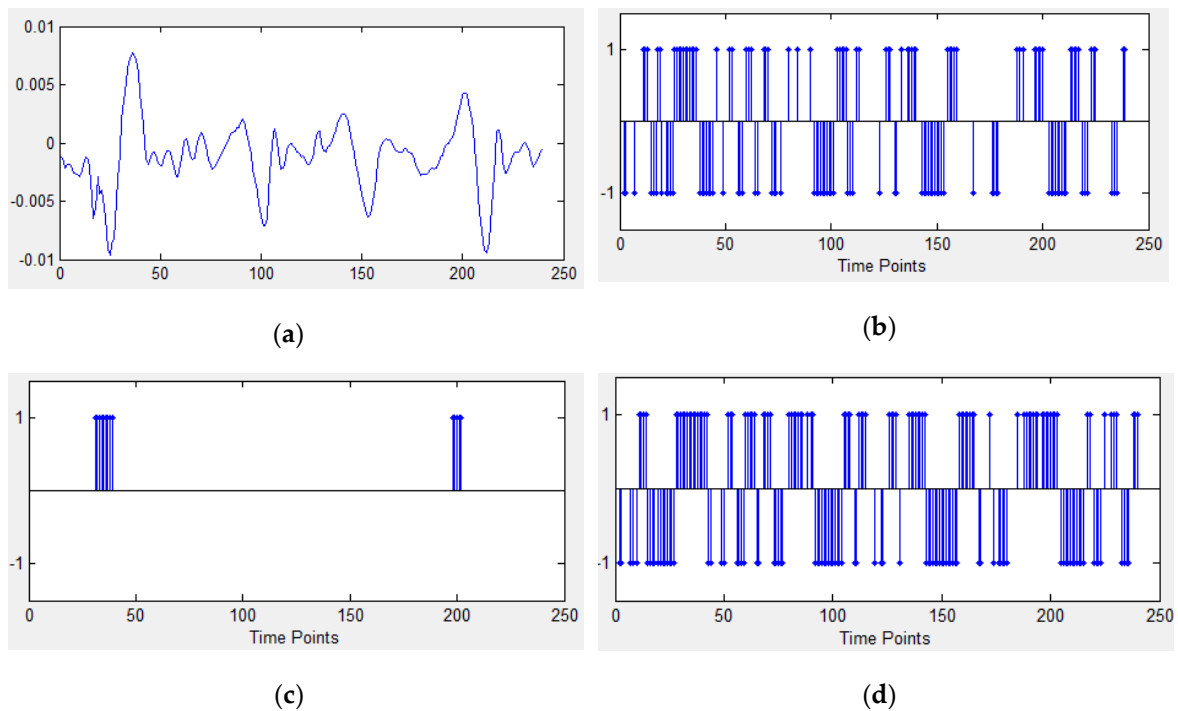
162 3.3. Structure damage classification

163 Temporal coding schemes such as Address event representation (AER), Bens spike algorithm
 164 (BSA) and step forward (SF) are used to represent information as an input to SNNs. Figure 2 shows
 165 different encoding results for the same temporal input data. The spike trains will carry key
 166 information of the original signals. Different spike encoding algorithms have distinct characteristics
 167 when representing input data. BSA, shown in Figure 2 (c), is suitable for high frequency signals, so
 168 there are few spikes encode from the low frequency signals, while AER and SF are better to represent
 169 the signal intensity.

170 Different spiking neuron models can be used to model spike generations at different description
 171 levels of biology [9], such as leaky integrate-and-fire (LIF), Izhikevich and Hodgkin–Huxley. The LIF
 172 neuron is one of the simplified models, which can be modelled as:

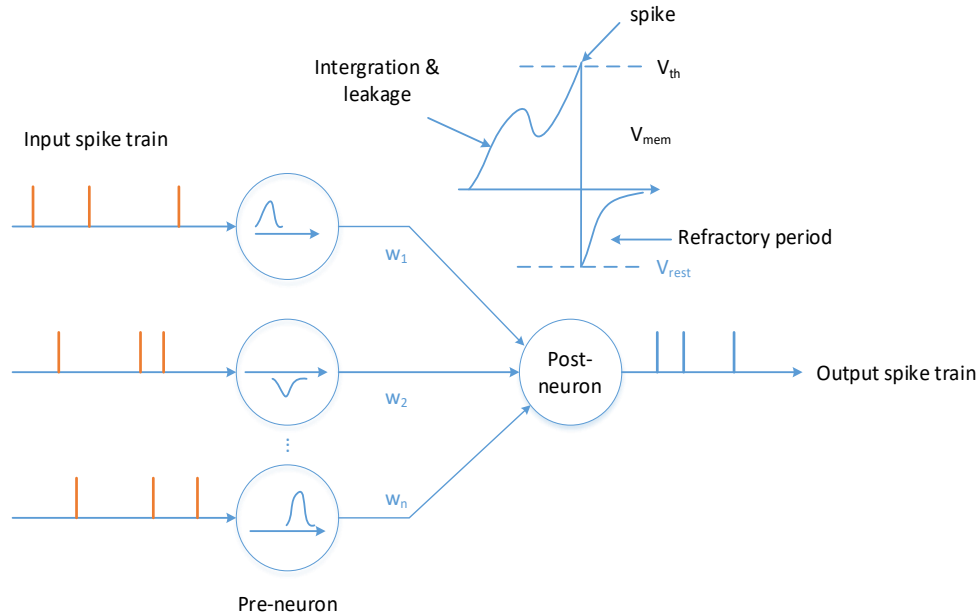
$$\tau_m \frac{dV_{mem}}{dt} = -(V_{mem} - V_{eq}) + RI^{ext} \quad (4)$$

173 where V_{mem} is the membrane potential of the neuron, I^{ext} is the external driving current, τ_m is the
 174 membrane time constant, R is the input resistance, and V_{eq} is the equilibrium potential of the leakage
 175 conductance.



176 **Figure 2.** Spike trains generated by three different coding schemes. (a) Data stream of a channel; (b)
 177 Encoding with AER; (c) Encoding with BSA; (d) Encoding with SF. Note that spikes in (b), (d) are
 178 positive or negative, but there are only positive spikes in (c).

179 Figure 3 shows the state of the neuron updated by the membrane potential under the synaptic
 180 stimuli. When the membrane potential of the neuron crosses the threshold, the neuron then generates
 181 an output spike, which acts as an input stimulus for subsequent layer neurons.



182

183

Figure 3. SNN neuron and computation model

184

185

186

SNN can be trained using unsupervised and supervised approaches. An unsupervised SNN using the Spike Timing Dependent Plasticity (STDP) learning rule was demonstrated with a competitive accuracy [31]. The weight update in STDP learning rule [32] can be described as:

$$\Delta w = \begin{cases} \alpha_+ e^{-\Delta t / \tau_+} & \Delta t \geq 0 \\ \alpha_- e^{\Delta t / \tau_-} & \Delta t < 0 \end{cases} \quad (5)$$

187

188

189

190

191

where Δw is the weight change rate, τ_+ and τ_- are STDP time constants, $\alpha_+ (> 0)$ and $\alpha_- (< 0)$ are constant coefficients, and Δt is the time difference between a post-neuron and a pre-neuron spike. When $\Delta t \geq 0$, the synaptic plasticity is a long-term potentiation (LTP) process; otherwise it's a long-term depression process. Two different SNN structures are adopted in this study, where one is a fully connected SNN, and the other one is a model based on NeuCube [27].

192

193

194

195

196

197

198

199

200

201

202

For performance comparisons, commonly used classification algorithms of K-means and ANNs are also used in this work for benchmarking. A supervised learning algorithm of ANN is used in this work, where the network weights are adjusted in every iteration by comparing difference between actual output and the targeted output. A multi-layer feedforward architecture with input layer for sensory input, hidden layer for learning and an output layer to generate spiking output. The number of input neurons equals to the number of sensors whereas output layer neurons represent number of structure level classifiers. For K-means, the unsupervised K-means algorithm for SHM can be described with the following steps where k is the number of desired clusters: (a). Given features' matrix as input, find the k centroids (random or select); (b). Calculate the distances between features' vectors and centroids; (c). Group the features' vectors based on their intra-cluster distance; and (d). Iterate the algorithm and update the centroids for a better clustering result.

203

4. Experiments

204

205

206

This section explains experimental setup to generate damage level report for SHM system. Furthermore, this case study analyses and compares results of three classification methods, K-means, ANN and SNN to identify best performing SHM system.

207

4.1. Dataset

208

209

This case study used a full-scale seven-story reinforced concrete building dataset for experimentation [1]. The building is installed with 45 accelerometers operating at sampling rate of

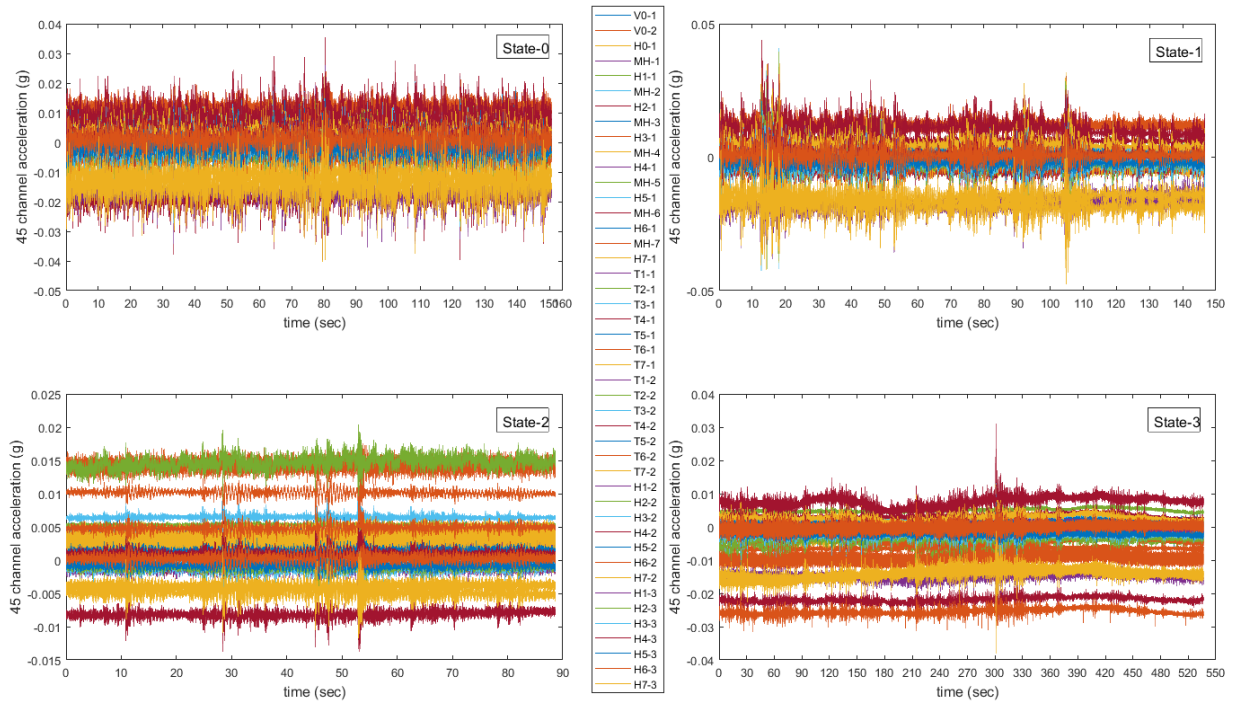
210 240Hz. A sequence of dynamic tests was applied to the building in several months, including ambient
 211 vibration tests, free vibration tests, and forced vibration tests using the UCSD-NEES shake table. A
 212 0.03g root-mean-square (RMS) acceleration white noise base excitation and an ambient vibration tests
 213 were performed on the structure before and between earthquake shake-table tests. For 45 channels,
 214 signal to noise ratios (SNR) are -36.97db~22.81db. The building was damaged progressively through
 215 several historical earthquake ground motions, and damage states of the building can be described as
 216 shown in Table 1. In 1st to 3rd earthquakes, the roof drift ratio, defined as the ratio between the
 217 maximum lateral displacement at the roof level of the building and the height of the roof relative to
 218 the base of the building, was measured as 0.28, 0.75 and 0.83%, respectively. The maximum tensile
 219 strain in the longitudinal reinforcing steel was measured close to the base of the wall as 0.61, 1.73 and
 220 1.78%, respectively [1].

221 **Table 1.** Dynamic tests used in this study

| Damage state | Description |
|--------------|---|
| State-0 | 8 min white noise base excitation process & 3 min ambient vibration |
| State-1 | After the 1 st earthquake excitation, with 8 min white noise base excitation process & 3 min ambient vibration |
| State-2 | After the 2 nd earthquake excitation, with 8 min white noise base excitation process & 3 min ambient vibration |
| State-3 | After the 3 rd earthquake excitation, with 8 min white noise base excitation process & 3 min ambient vibration |

222 4.2. Feature extraction

223 The raw data collected from 45 channels in the building at different health states are shown in
 224 Figure 4. Raw accelerometer data of different structure states show different features, such as
 225 maximum amplitude and mean value etc. By considering the building physical movements in
 226 different states [33], the deformation degree of buildings can result in large differences in the mean
 227 and fluctuation range of accelerometer data. Based on these analysis, zero-crossing rate, mean and
 228 variance are used for feature extractions.



229

230

Figure 4. Row data from 45-channel accelerometers

231

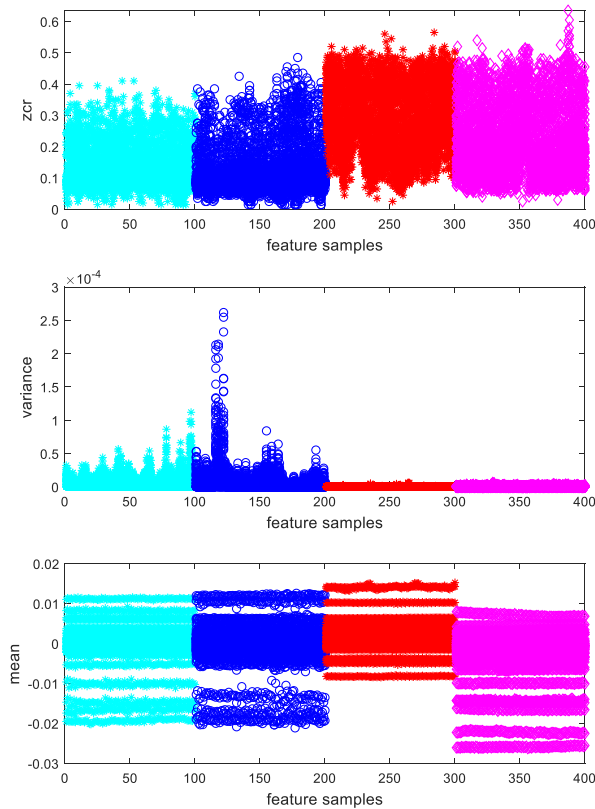
After the data has been pre-processed, three methods (including zero-crossing rate, variance and mean value) are used to extract data in order to select the damage-sensitive features. The features are presented in Figure 5. The zero-crossing rate, which is the rate of sign-changes along a signal, is weak to separate the different damage states (indicated by colors). Among them, calculating mean value of sensor data has the potential to differentiate the four damage states.

232

233

234

235



236

237 **Figure 5.** Results of the features extracted from raw data

238 4.3. SHM classification results

239 For different classification methods, 70%–80% samples (including mean samples and raw
240 data) are used for training, and the rest for validation and testing.

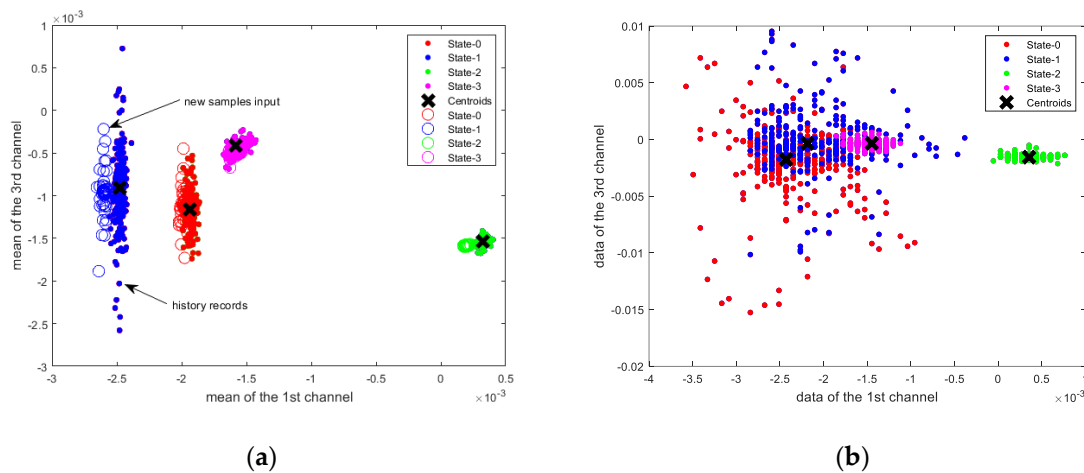
241 4.3.1. K-means

242 A 50 step-length sliding window with 100 sample points is used to get more mean samples,
243 which are used as input for the k-means algorithm. K-means parameters are shown in table 2.

244 **Table 2.** Parameters in k-means

| Parameters setting | Cluster number | Distance | Initial centroid positions | Replicates |
|--------------------|----------------|-------------|----------------------------|------------|
| | 4 | L1 distance | Random | 8 |

245 It can be seen from Figure 6 (a) that using the mean value of the data as an input of the k-means
246 algorithm can classify the health status of the building. The dots represent historical records and the
247 circles represent new data inputs. The classification accuracy of structural health status is 100%. In
248 Figure 6 (b), the raw data are used directly as the input of the k-means algorithm. In the case of
249 overlapped data, including State-0, State-1 and State-3, the k-means algorithm cannot separate these
250 data. There are 45 channels in total and only two of them are used for the demonstration in Figure 6.



251 **Figure 6.** SHM classification using K-means. (a) Clustering of mean samples; (b) Clustering of raw data.

252 By incorporating hardware design process [34] to implement K-means, the input data dimension
253 area will be about 3.46 mm^2 and 1.23 mm^2 for parallel mode and multiplexed architecture
254 respectively.

255 4.3.2. ANN

256 The ANN with 45 input neurons, 20 hidden neurons and 4 output neurons can get similar
257 accuracy with different input samples (mean samples and raw data). Table 3 shows that ANN slightly
258 confuse between State-0 and State-1 when trained on raw data samples. The hardware area of the
259 neuron is estimated about 1.347 mm^2 based on a 45nm CMOS technology [35]. It can also be calculated
260 from [36] that the total hardware area of ANN is >0.798 mm^2 .

261 **Table 3.** Classification matching matrix with different input samples

262

(a) Mean samples

| Predict label \ True label | State-0 | State-1 | State-2 | State-3 |
|----------------------------|---------|---------|---------|---------|
| | State-0 | 100% | 0.0% | 0.0% |
| State-1 | 0.0% | 100% | 0.0% | 0.0% |
| State-2 | 0.0% | 0.0% | 100% | 0.0% |
| State-3 | 0.0% | 0.0% | 0.0% | 100% |

263

(b) Raw data

| Predict label \ True label | State-0 | State-1 | State-2 | State-3 |
|----------------------------|---------|---------|---------|---------|
| | State-0 | 99.7% | 0.3% | 0.0% |
| State-1 | 0.9% | 99.1% | 0.0% | 0.0% |
| State-2 | 0.0% | 0.0% | 100% | 0.0% |
| State-3 | 0.0% | 0.0% | 0.0% | 100% |

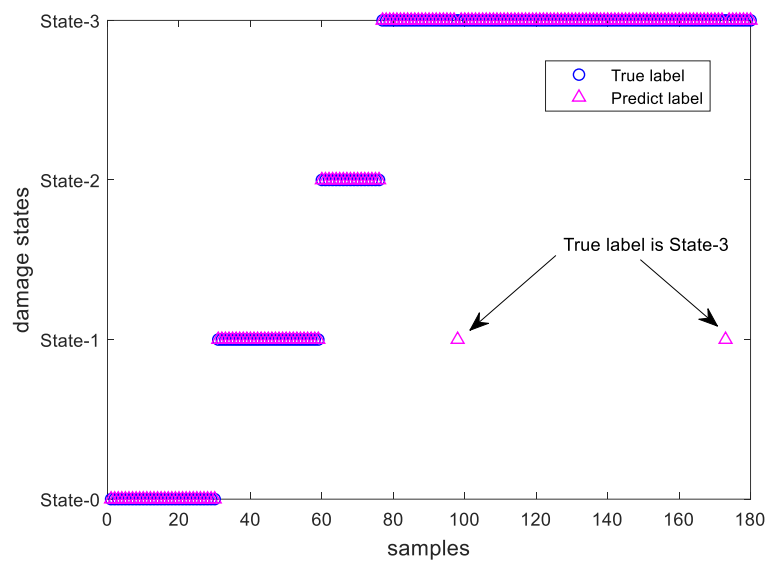
264 4.3.3. NeuCube

265 In NeuCube, raw data samples are fed into a dynamic SNN. One channel of an input sample
 266 was shown in Figure 2(a). Table 4 shows network parameters used by NeuCube. The model is
 267 established with 45 input neurons, 50 hidden neurons and output neurons (the number of samples).
 268 Due to the dynamic structure, the overall area overhead of NeuCube SNN is about $4.655 \times 10^{-3} \text{mm}^2$
 269 that is calculated according to neuronal and synaptic hardware area estimation proposed in [37,38].
 270 Results shows that overall classification accuracy of NeuCube SNN is 98.9% (as shown in Figure 7).

271

Table 4. NeuCube Model Parameter Setting

| Parameter | Description | Value |
|-----------------------------|--|----------|
| STDP Rate | Defines the learning rate of the STDP learning | 0.01 |
| Firing threshold | Defines the threshold membrane potential beyond which the neuron fires a spike. | 0.5 |
| deSNN Classifier Parameters | The weight is calculated as a modulation factor (the variable mod) to the power of the order of the incoming spikes. | 0.55-0.6 |
| Drift | Initial connection weights are further modified to reflect the following spikes, using a drift parameter. | 0.015 |



272

273

Figure 7. Classification result by using NeuCube (raw data)

274

275 Table 5 shows breakdown of performance accuracy for classification of damage states observed
 276 by NeuCube. Enough samples will contribute to higher probability of making correct decision about
 277 the damage states. As a comparison, mean samples are input into NeuCube with the same parameter
 278 setting above. The accuracy is not as stable as raw data input, as NeuCube is more sensitive to
 279 temporal raw data [39].

280

Table 5. Accuracy of each class

| Damage state | Accuracy |
|--------------|----------|
| State-0 | 100% |
| State-1 | 100% |
| State-2 | 100% |
| State-3 | 98.08% |

281 4.3.4. Customized SNN

282 A customized fully connected SNN with LIF neurons and SpikeProp as learning algorithm is
 283 developed for the SHM classification based on previous work [40]. The three-layered fully connected
 284 SNN is designed and modelled in MATLAB. Table 6 shows network topology, size and hardware
 285 area of LIF based SNN model. Mean sensory samples are fed through 45 spiking input neurons to
 286 propagate spike towards 10 hidden neurons in order to generate 4 state output at 1 output neuron.
 287 The estimated hardware area of the SNN chip shown in Table 6 is calculated using [37,38].

288

Table 6. SNN setting and result (mean samples)

| Network | Topology | Multiplier of synapses | Total neurons | Total synapses |
|---------|-----------|------------------------|---------------|----------------|
| SNN | [45:10:1] | 10 | 56 | 460 |

| Area of neurons | Area of synapses | Area overhead | Overall Accuracy | Number of iterations |
|------------------------------------|------------------------------------|------------------------------------|------------------|----------------------|
| $5.04 \times 10^{-4} \text{ mm}^2$ | $1.10 \times 10^{-3} \text{ mm}^2$ | $1.61 \times 10^{-3} \text{ mm}^2$ | 99.18% | 2500 |
| | | | 99.46% | 3000 |

289 Damage states are encoded with time of spike of output neuron (SNN output). Experimentation
 290 results shows the classification accuracy using mean samples input. Results shows in Table 7 that
 291 proposed customized SNN classifies structural damage with 99.18% accuracy for mean dataset.
 292 Moreover, the overall accuracy can be higher to 99.46% by increasing number of iterations, as
 293 compared to 98.9% NeuCube average accuracy for raw sensory input.

294

Table 7. Accuracy of each class

| Damage state | SNN output | Accuracy | Accuracy |
|-------------------------|------------|----------|----------|
| State-0 | 16 | 100% | 100% |
| State-1 | 18 | 95.67% | 97% |
| State-2 | 20 | 100% | 100% |
| State-3 | 22 | 99.8% | 99.9% |
| Overall accuracy | | 99.18% | 99.46% |

295 4.3.5. Discussions

296 A summary of results using K-means, ANN and SNN in SHM applications, is shown in Table 8.
 297 ANN used raw data and feature samples as input, and there is little difference in classification
 298 accuracy. The final decision making can be the same within a certain confidence interval. Thus, if
 299 ANN combines the feature extraction into the learning process, it improves the computing speed,
 300 and also reduces the hardware consumption. The structural damage occurrence detection can be
 301 assessed as health (State-0) and damage (State-1, State-2 & State-3), then the sensitivity (true positive
 302 rate) and specificity (true negative rate) of three typical methods can be obtained with the input of
 303 raw data samples, as shown in Table 9. Compared with other two algorithms, SNN can accurately
 304 determine whether the structure is healthy. Meanwhile, the hardware area consumption of SNN is
 305 much less than ANN, the classification accuracy has a little difference of 0.9%, and the sensitivity and
 306 specificity are higher. In summary, the proposed method based on SNNs apparently achieves a good
 307 trade-off between classification, reliability, and hardware resource consumption.

308

Table 8. Performance comparison of three methods in SHM application

| Method | Classification accuracy | | Technology | Hardware area |
|---------|-------------------------|---------|------------|--|
| | Raw data | Feature | | |
| K-means | 80% | 100% | TSMC 90nm | $1.23 \text{ mm}^2 \sim 3.46 \text{ mm}^2$ |
| ANN | 99.8% | 100% | CMOS 45nm | 1.347 mm^2 (neurons only) |
| SNN | 98.9% | 99.46% | CMOS 90nm | $4.655 \times 10^{-3} \text{ mm}^2$ (NeuCube) $1.61 \times 10^{-3} \text{ mm}^2$ (Customized SNN) |

309

Table 9. Sensitivity and specificity comparison of three methods

| Method | Sensitivity | Specificity |
|---------|-------------|-------------|
| K-means | 92.97% | 73.87% |
| ANN | 99.94% | 99.15% |
| SNN | 100% | 100% |

310 5. Conclusions

311 The structural health state detection in this study involves the feature extraction from
 312 periodically observation measurements of a structure, where these features are analysed to determine
 313 the current health state of the structure. Based on the detected states, appropriate repair and
 314 strengthening of structures can keep the structure operational and longeval. Through the analysis of
 315 ZCR, Mean and Variance of the raw sensor data, it is found by experiments that mean value is more
 316 sensitive to the structure state. Therefore, mean values and raw data were used as inputs, and several
 317 classification methods, including K-means, conventional ANN and SNN, were used to detect the
 318 health state of the structure. Analysis and comparison results show that the SNN algorithm proposed
 319 in this study has advantages including (a). High classification accuracy can be obtained by directly
 320 using the raw data as input without manual feature extraction; (b). The small part of misclassification
 321 (1.92%) only exists in State-3, where the output health states can be clearly distinguished; (c). The
 322 hardware area of SNN is lower compared to ANN or K-means. **In summary, the proposed SNN
 323 hardware solution for SHM has a stronger survivability and reliability than conventional approaches.
 324 Further work will further optimize the SNN for SHM systems from two aspects including a). to
 325 develop multi-layer (deep) SNNs to improve the accuracy, and b). to further analyze the sensor data
 326 to enhance the system functionalities, such as reporting the location of damage or life forecast of the
 327 structure.**

328 **Author Contributions:** Conceptualization, Jim Harkin and Junxiu Liu; Methodology, Jim Harkin and Junxiu
 329 Liu; Investigation, George Martin; Software, Lili Pang and Aqib Javed; Validation, Lili Pang, Aqib Javed,
 330 Malachy McElholm and Liam McDaid; Formal analysis, Malachy McElholm; Writing—original draft
 331 preparation, Lili Pang; Writing—review and editing, Lili Pang, Junxiu Liu, Jim Harkin, George Martin, Malachy
 332 McElholm, Aqib Javed and Liam McDaid. All authors have read and agreed to the published version of the
 333 manuscript.

334 **Conflicts of Interest:** The authors declare no conflict of interest.

335 References

- 336 1. Moaveni, B.; He, X.; Conte, J.P.; Restrepo, J.I.; Panagiotou, M. System identification study of a 7-story full-
 337 scale building slice tested on the UCSD-NEES shake table. *J. Struct. Eng.* **2011**, doi:10.1061/(ASCE)ST.1943-
 338 541X.0000300.
- 339 2. Park, S.W.; Park, H.S.; Kim, J.H.; Adeli, H. 3D displacement measurement model for health monitoring of
 340 structures using a motion capture system. *Meas. J. Int. Meas. Confed.* **2015**,
 341 doi:10.1016/j.measurement.2014.09.063.
- 342 3. Hernandez, E.; Roohi, M.; Rosowsky, D. Estimation of element-by-element demand-to-capacity ratios in
 343 instrumented SMRF buildings using measured seismic response. *Earthq. Eng. Struct. Dyn.* **2018**,
 344 doi:10.1002/eqe.3099.
- 345 4. Hsu, T.Y.; Yin, R.C.; Wu, Y.M. Evaluating post-earthquake building safety using economical MEMS
 346 seismometers. *Sensors (Switzerland)* **2018**, doi:10.3390/s18051437.
- 347 5. Abdo, M. *Structural Health Monitoring, History, Applications and Future. A Review Book*; 2014; ISBN 978-1-
 348 941926-07-9.

- 349 6. Liu, J.; McDaid, L.J.; Harkin, J.; Karim, S.; Johnson, A.P.; Millard, A.G.; Hilder, J.; Halliday, D.M.; Tyrrell,
350 A.M.; Timmis, J. Exploring Self-Repair in a Coupled Spiking Astrocyte Neural Network. *IEEE Trans. Neural*
351 *Networks Learn. Syst.* **2019**, doi:10.1109/TNNLS.2018.2854291.
- 352 7. Liu, J.; McDaid, L.J.; Harkin, J.; Wade, J.J.; Karim, S.; Johnson, A.P.; Millard, A.G.; Halliday, D.M.; Tyrrell,
353 A.M.; Timmis, J. Self-repairing learning rule for spiking astrocyte-neuron networks. In Proceedings of the
354 Lecture Notes in Computer Science (including subseries Lecture Notes in Artificial Intelligence and Lecture
355 Notes in Bioinformatics); 2017.
- 356 8. Lee, J.H.; Delbruck, T.; Pfeiffer, M. Training deep spiking neural networks using backpropagation. *Front.*
357 *Neurosci.* **2016**, doi:10.3389/fnins.2016.00508.
- 358 9. Roy, K.; Jaiswal, A.; Panda, P. Towards spike-based machine intelligence with neuromorphic computing.
359 *Nature* **2019**, doi:10.1038/s41586-019-1677-2.
- 360 10. Bull, L.A.; Rogers, T.J.; Wickramarachchi, C.; Cross, E.J.; Worden, K.; Dervilis, N. Probabilistic active
361 learning: An online framework for structural health monitoring. *Mech. Syst. Signal Process.* **2019**,
362 doi:10.1016/j.ymssp.2019.106294.
- 363 11. Eftekhar Azam, S.; Rageh, A.; Linzell, D. Damage detection in structural systems utilizing artificial neural
364 networks and proper orthogonal decomposition. *Struct. Control Heal. Monit.* **2019**, doi:10.1002/stc.2288.
- 365 12. Worden, K.; Manson, G. The application of machine learning to structural health monitoring. *Philos. Trans.*
366 *R. Soc. A Math. Phys. Eng. Sci.* **2007**, doi:10.1098/rsta.2006.1938.
- 367 13. Amezcua-Sanchez, J.P.; Adeli, H. Feature extraction and classification techniques for health monitoring
368 of structures. *Sci. Iran.* 2015.
- 369 14. Bouzenad, A.E.; Mountassir, M. El; Yaacoubi, S.; Dahmene, F.; Koabaz, M.; Buchheit, L.; Ke, W. A semi-
370 supervised based k-means algorithm for optimal guided waves structural health monitoring: A case study.
371 *Inventions* **2019**, doi:10.3390/inventions4010017.
- 372 15. Amezcua-Sanchez, J.P.; Valtierra-Rodriguez, M.; Adeli, H. Wireless smart sensors for monitoring the
373 health condition of civil infrastructure. *Sci. Iran.* 2018.
- 374 16. Karayannis, C.G.; Chalioris, C.E.; Angeli, G.M.; Papadopoulos, N.A.; Favvata, M.J.; Providakis, C.P.
375 Experimental damage evaluation of reinforced concrete steel bars using piezoelectric sensors. *Constr. Build.*
376 *Mater.* **2016**, doi:10.1016/j.conbuildmat.2015.12.019.
- 377 17. Oh, B.K.; Kim, K.J.; Kim, Y.; Park, H.S.; Adeli, H. Evolutionary learning based sustainable strain sensing
378 model for structural health monitoring of high-rise buildings. *Appl. Soft Comput. J.* **2017**,
379 doi:10.1016/j.asoc.2017.05.029.
- 380 18. Jang, S.; Jo, H.; Cho, S.; Mechtov, K.; Rice, J.A.; Sim, S.H.; Jung, H.J.; Yun, C.B.; Spencer, B.F.; Agha, G.
381 Structural health monitoring of a cable-stayed bridge using smart sensor technology: Deployment and
382 evaluation. *Smart Struct. Syst.* **2010**, doi:10.12989/sss.2010.6.5_6.439.
- 383 19. Wang, J.F.; Xu, Z.Y.; Fan, X.L.; Lin, J.P. Thermal Effects on Curved Steel Box Girder Bridges and Their
384 Countermeasures. *J. Perform. Constr. Facil.* **2017**, doi:10.1061/(ASCE)CF.1943-5509.0000952.

- 385 20. Mesquita, E.; Arêde, A.; Pinto, N.; Antunes, P.; Varum, H. Long-term monitoring of a damaged historic
386 structure using a wireless sensor network. *Eng. Struct.* **2018**, doi:10.1016/j.engstruct.2018.02.013.
- 387 21. Notley, S.; Magdon-Ismail, M. Examining the Use of Neural Networks for Feature Extraction: A
388 Comparative Analysis using Deep Learning, Support Vector Machines, and K-Nearest Neighbor Classifiers
389 2018.
- 390 22. Zhang, Y.Z.; Hu, X.F.; Zhou, Y.; Duan, S.K. A Novel Reinforcement Learning Algorithm Based on
391 Multilayer Memristive Spiking Neural Network With Applications. *Zidonghua Xuebao/Acta Autom. Sin.*
392 **2019**, doi:10.16383/j.aas.c180685.
- 393 23. Naeem, M.; McDaid, L.J.; Harkin, J.; Wade, J.J.; Marsland, J. On the Role of Astroglial Syncytia in Self-
394 Repairing Spiking Neural Networks. *IEEE Trans. Neural Networks Learn. Syst.* **2015**,
395 doi:10.1109/TNNLS.2014.2382334.
- 396 24. Gonzalez, I.; Khouri, E.; Gentile, C.; Karoumi, R. Novel AI-based railway SHM, its behaviour on simulated
397 data versus field deployment. In Proceedings of the Proceedings of the 7th Asia-Pacific Workshop on
398 Structural Health Monitoring, APWSHM 2018; 2018.
- 399 25. Medhi, M.; Dandautiya, A.; Raheja, J.L. Real-Time Video Surveillance Based Structural Health Monitoring
400 of Civil Structures Using Artificial Neural Network. *J. Nondestruct. Eval.* **2019**, doi:10.1007/s10921-019-0601-
401 x.
- 402 26. de Oliveira, M.A.; Araujo, N.V.S.; da Silva, R.N.; da Silva, T.I.; Epaarachchi, J. Use of Savitzky-Golay filter
403 for performances improvement of SHM systems based on neural networks and distributed PZT sensors.
404 *Sensors (Switzerland)* **2018**, doi:10.3390/s18010152.
- 405 27. Kasabov, N.K.; Dobarjeh, M.G.; Dobarjeh, Z.G. Mapping, learning, visualization, classification, and
406 understanding of fMRI Data in the NeuCube evolving spatiotemporal data machine of spiking neural
407 networks. *IEEE Trans. Neural Networks Learn. Syst.* **2017**, doi:10.1109/TNNLS.2016.2612890.
- 408 28. Kasabov, N.; Dhoble, K.; Nuntalid, N.; Indiveri, G. Dynamic evolving spiking neural networks for on-line
409 spatio- and spectro-temporal pattern recognition. *Neural Networks* **2013**, doi:10.1016/j.neunet.2012.11.014.
- 410 29. Ghosh-Dastidar, S.; Adeli, H. Spiking neural networks. *Int. J. Neural Syst.* **2009**,
411 doi:10.1142/S0129065709002002.
- 412 30. Benjamin, B.V.; Gao, P.; McQuinn, E.; Choudhary, S.; Chandrasekaran, A.R.; Bussat, J.M.; Alvarez-Icaza,
413 R.; Arthur, J. V.; Merolla, P.A.; Boahen, K. Neurogrid: A mixed-analog-digital multichip system for large-
414 scale neural simulations. *Proc. IEEE* **2014**, doi:10.1109/JPROC.2014.2313565.
- 415 31. Diehl, P.U.; Cook, M. Unsupervised learning of digit recognition using spike-timing-dependent plasticity.
416 *Front. Comput. Neurosci.* **2015**, doi:10.3389/fncom.2015.00099.
- 417 32. Higgins, I.; Stringer, S.; Schnupp, J. Unsupervised learning of temporal features for word categorization in
418 a spiking neural network model of the auditory brain. *PLoS One* **2017**, doi:10.1371/journal.pone.0180174.
- 419 33. Moaveni, B.; He, X.; Conte, J.P.; Restrepo, J.I. Damage identification study of a seven-story full-scale
420 building slice tested on the UCSD-NEES shake table. *Struct. Saf.* **2010**, doi:10.1016/j.strusafe.2010.03.006.

- 421 34. Chen, T.W.; Chien, S.Y. Bandwidth adaptive hardware architecture of K-Means clustering for intelligent
422 video processing. In Proceedings of the ICASSP, IEEE International Conference on Acoustics, Speech and
423 Signal Processing - Proceedings; 2009.
- 424 35. Sun, Y.; Cheng, A.C. Machine learning on-a-chip: A high-performance low-power reusable neuron
425 architecture for artificial neural networks in ECG classifications. *Comput. Biol. Med.* **2012**,
426 doi:10.1016/j.combiomed.2012.04.007.
- 427 36. Wang, L.; Liu, S.; Lu, C.; Zhang, L.; Xiao, J.; Wang, J. Stable matching scheduler for single-ISA
428 heterogeneous multi-core processors. In Proceedings of the Lecture Notes in Computer Science (including
429 subseries Lecture Notes in Artificial Intelligence and Lecture Notes in Bioinformatics); 2015.
- 430 37. Harkin, J.; Morgan, F.; McDaid, L.; Hall, S.; McGinley, B.; Cawley, S. A Reconfigurable and Biologically
431 Inspired Paradigm for Computation Using Network-On-Chip and Spiking Neural Networks. *Int. J.*
432 *Reconfigurable Comput.* **2009**, doi:10.1155/2009/908740.
- 433 38. Liu, J.; Harkin, J.; McElholm, M.; McDaid, L.; Jimenez-Fernandez, A.; Linares-Barranco, A. Case study: Bio-
434 inspired self-adaptive strategy for spike-based PID controller. In Proceedings of the Proceedings - IEEE
435 International Symposium on Circuits and Systems; 2015.
- 436 39. Kasabov, N.; Scott, N.M.; Tu, E.; Marks, S.; Sengupta, N.; Capecci, E.; Othman, M.; Doborjeh, M.G.; Murli,
437 N.; Hartono, R.; et al. Evolving spatio-temporal data machines based on the NeuCube neuromorphic
438 framework: Design methodology and selected applications. *Neural Networks* **2016**,
439 doi:10.1016/j.neunet.2015.09.011.
- 440 40. Javed, A.; Harkin, J.; McDaid, L.J.; Liu, J. Exploring Spiking Neural Networks for Prediction of Traffic
441 Congestion in Networks-on-Chip.; 2020; pp. 1–5.

442



© 2020 by the authors. Submitted for possible open access publication under the terms and conditions of the Creative Commons Attribution (CC BY) license (<http://creativecommons.org/licenses/by/4.0/>).

443